Supporting Information for

Molecular Modifiers Suppress Nonclassical Pathways of Zeolite Crystallization

*Wei Qin, Ankur Agarwal, Madhuresh K. Choudhary, Jeremy C. Palmer, and Jeffrey D. Rimer**

Department of Chemical and Biomolecular Engineering, University of Houston, 4726 Calhoun Road, Houston, TX 77204 USA

*Correspondence sent to: jrimer@central.uh.edu

List of Figures

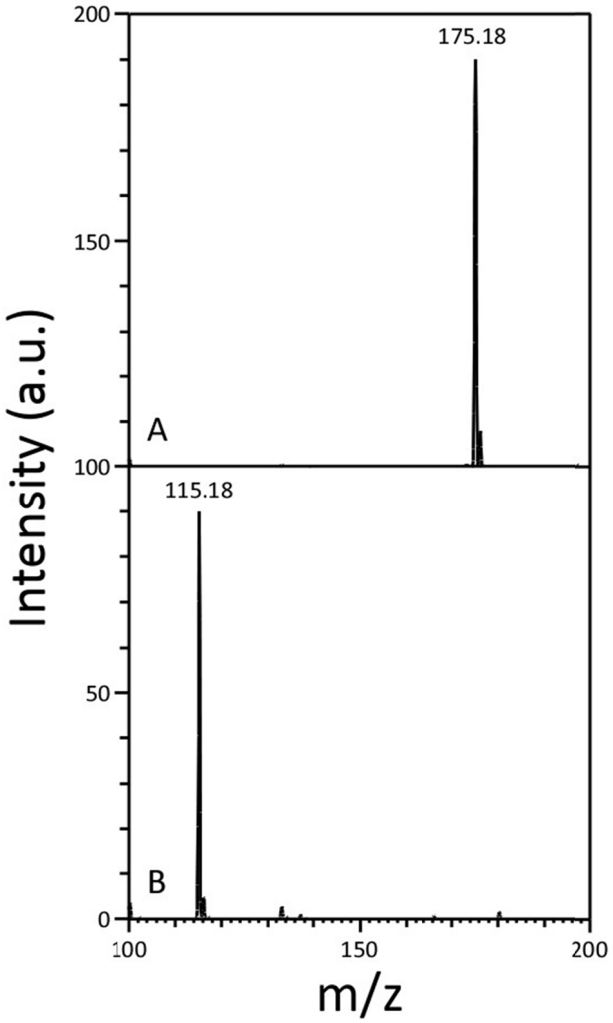

Figure S1. Mass spectra of a solution containing D-arginine and NaOH (pH 12.3) that was measured (A) before and (B) after hydrothermal treatment at 160°C for 72 h. The m/z ratios correspond to D-arginine and (R)-ornithine-lactam, respectively.

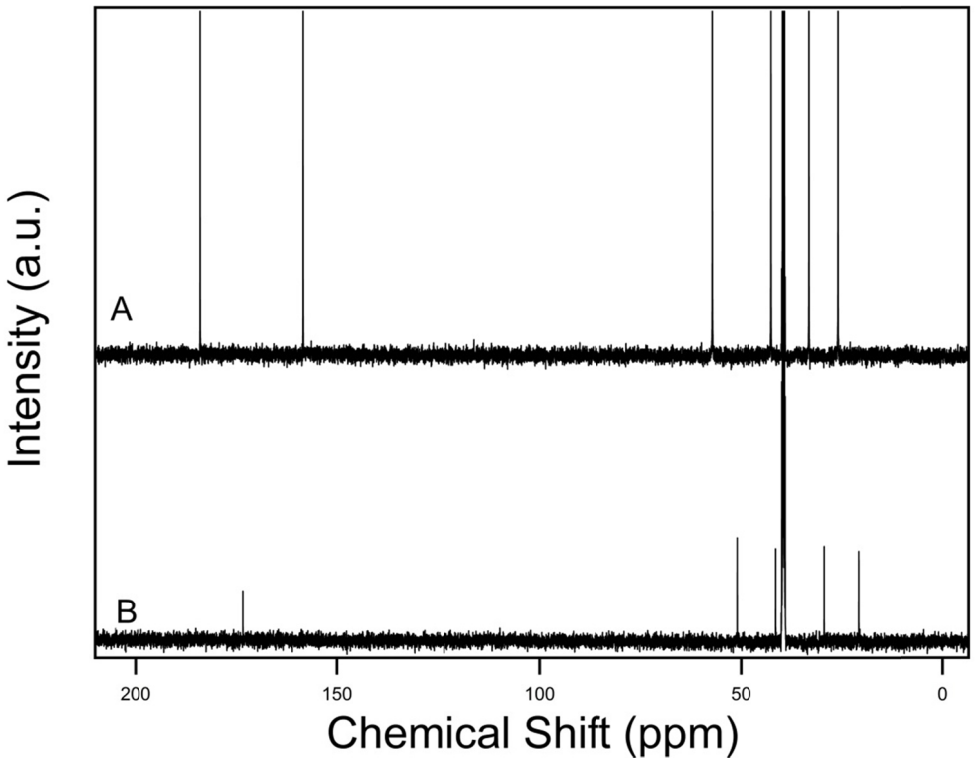

Figure S2. ^{13}C-NMR spectrum in DMSO of (A) D-Arg and (B) organics that were extracted from a solution containing D-arginine and NaOH (pH 12.3) after heating at 160°C for 72 h. The pattern matches that of ornithine-lactam (see Figure S3).

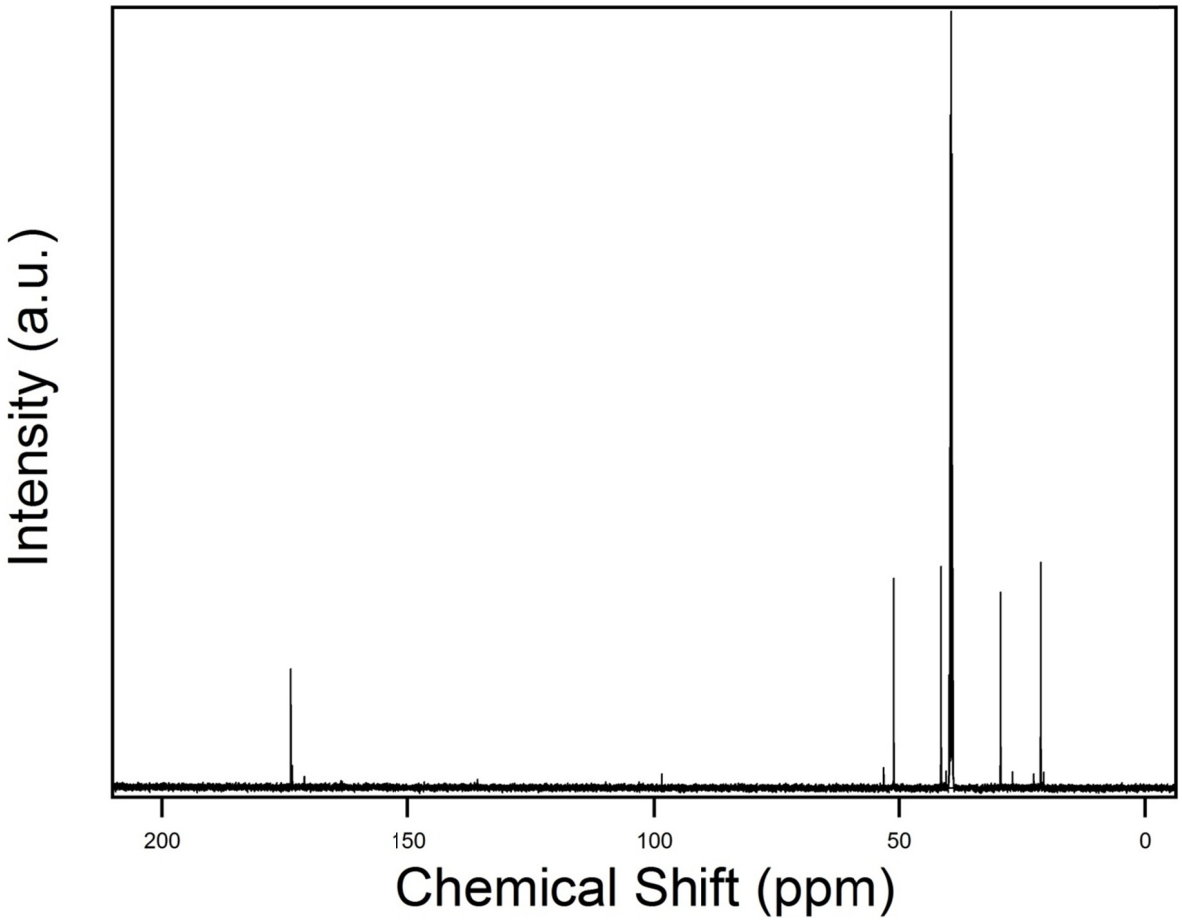

Figure S3. ^{13}C-NMR spectrum of ornithine-lactam (R/S-OL) in DMSO. The reagent was purchased from AK Scientific Inc. to confirm the product of D-Arg. thermal decomposition.

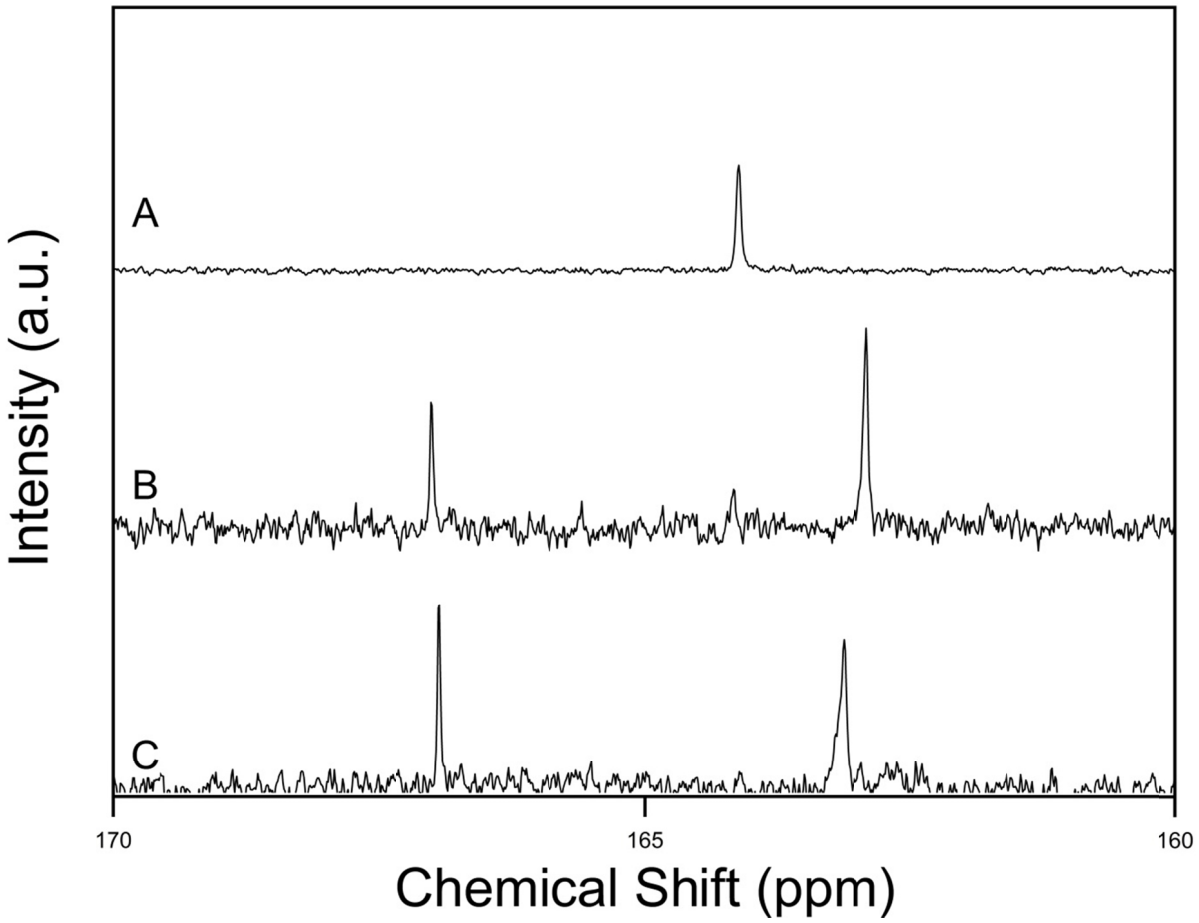

Figure S4. ^{13}C-NMR spectrum of urea measured in alkaline solution (A) without heating (i.e. as received reagent from EMD Chemicals Inc.), and after hydrothermal treatment at 160°C for (B) 4 h and (C) 8 h. The final product of urea decomposition is carbonate.

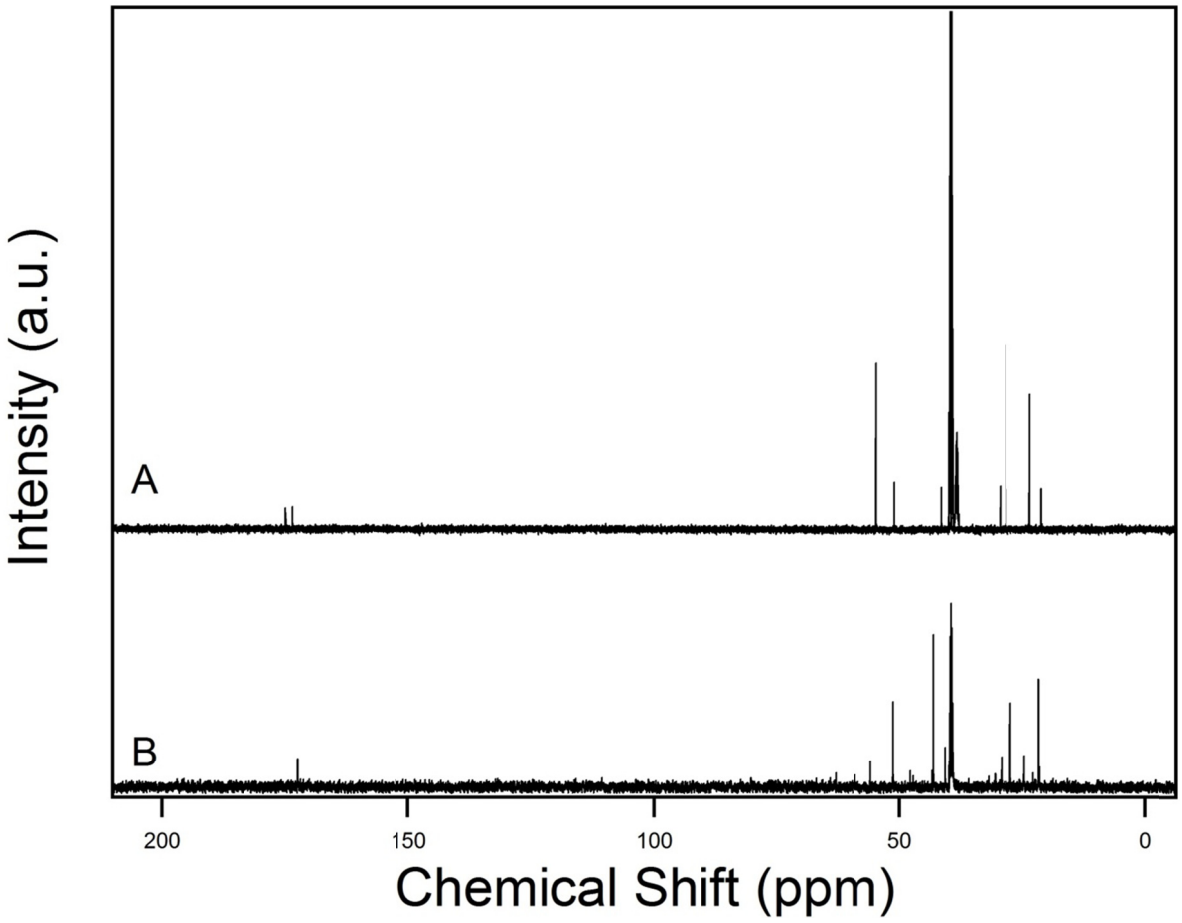

Figure S5. ^{13}C-NMR spectrum of D-ornithine measured in alkaline solution (A) without heating (i.e. as received reagent from Sigma Aldrich), and (B) after hydrothermal treatment at 160°C for 8 h. The pattern matches that of ornithine-lactam (see Figure S3).

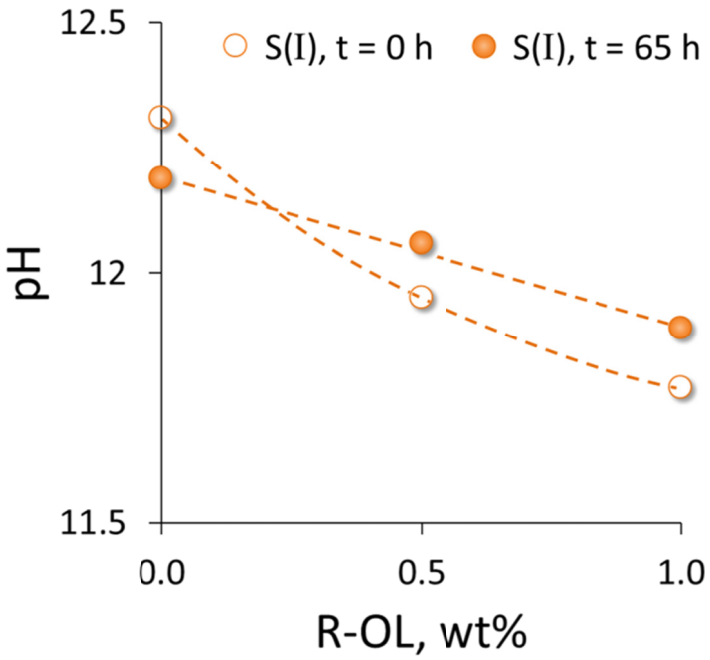

Figure S6. Measurements of pH for silicalite-1 growth solution S(I) prior to (pH_i, open symbols) and after (pH_o, solid symbols) hydrothermal treatment at 160°C for 65 h as a function of R-OL weight percentage. The dashed lines are interpolated to help guide the eye.

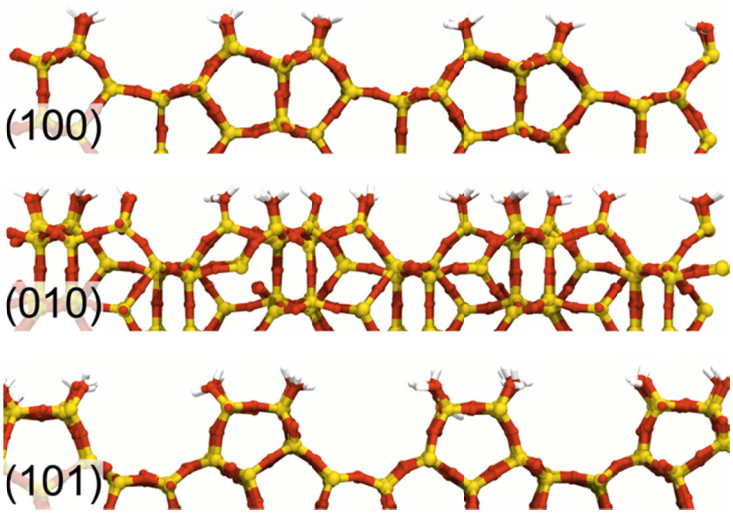

Figure S7. Model (hkl) surfaces of silicalite-1 used in the USMD simulations to investigate R/S-OL adsorption.

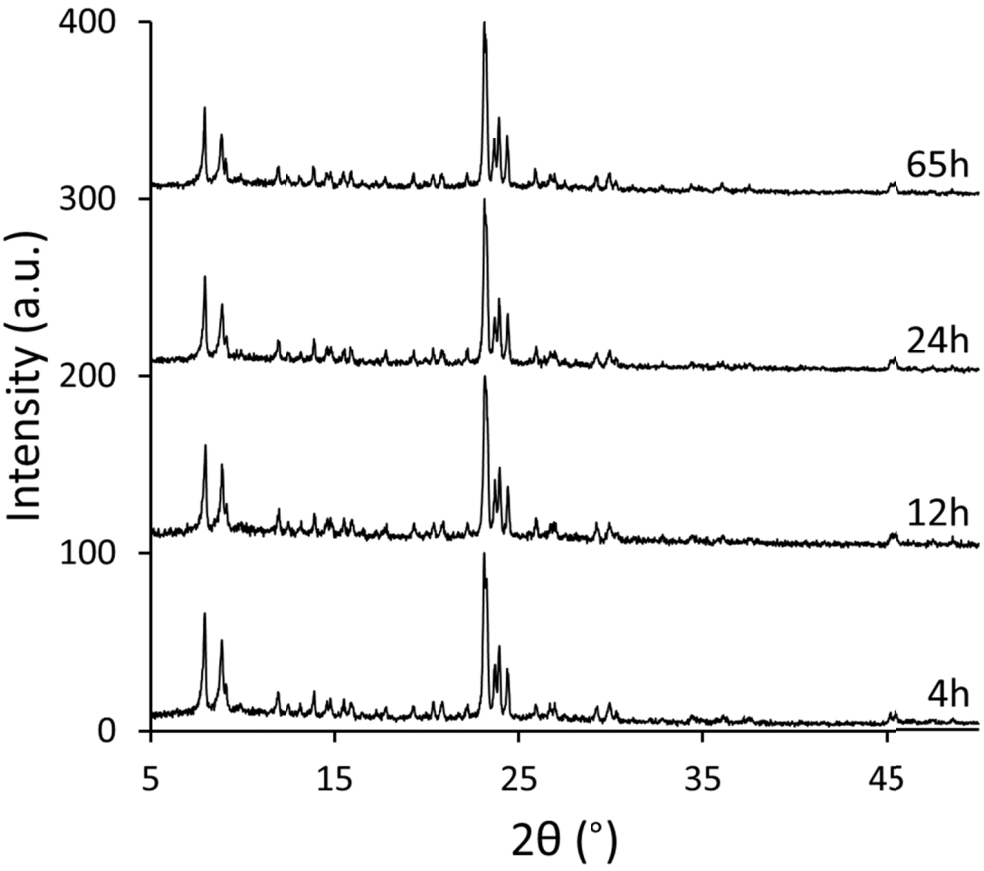

Figure S8. Powder XRD patterns of extracted solids from S(II) growth solutions after 4, 12, 24, and 65 h of hydrothermal treatment at 160°C.

Growth modification of ZSM-5. The effect of R-OL on ZSM-5 (MFI type) crystal morphology and size was assessed by bulk crystallization studies in both the absence of modifier and in the presence of varying R-OL weight fraction. We added aluminum sulfate ($Al_2(SO_4)_3$) to solution S(II)′ to make an initial gel Si/Al ratio of 50. The majority of aluminosilicate species are in the form of nanoparticle precursors. ZSM-5 crystals produced from growth solution S(II)′ (containing Al) in the absence of modifier exhibit a typical ZSM-5 morphology (Figure S9A). A systematic study of varying modifier content (Figure S9C) reveals little change in crystal thickness, while crystal length increases monotonically with increasing D-Arg concentration. The aspect ratio of length over thickness increases with increasing modifier concentration (Figure S9B). This agrees with the observations for silicalite-1 crystals synthesized in solution S(II).

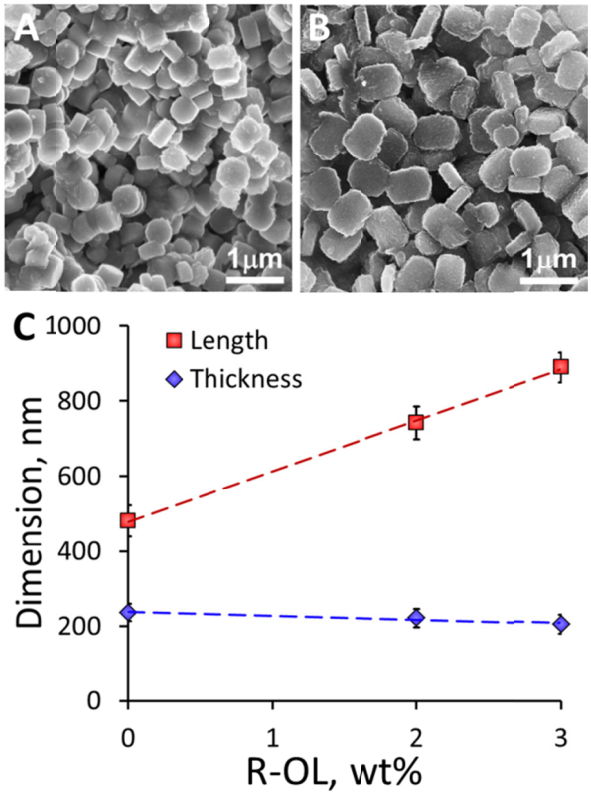

Figure S9. Effect of R-OL (i.e. the decomposition product of D-Arg) on the morphology of ZSM-5 crystals synthesized from growth solutions with molar composition 157 SiO_2:1.57 Al_2O_3:47 TPAOH. Scanning electron micrographs of ZSM-5 crystals prepared with the following synthesis conditions: (A) control (absence of D-Arg) and (B) 3 wt% D-Arg. (C) Plot of crystal length (red squares) and thickness (blue triangles) of ZSM-5 crystals as a function of modifier concentration. Crystal dimensions are obtained from SEM images and each value is the

average of more than 50 measurements from a single crystal batch. Dashed lines are interpolated to help guide the eye, and error bars equal two standard deviations.